

Future flow and water temperature scenarios in an impounded drainage basin: Implications for summer flow and temperature management downstream of the dam

Mostafa Khorsandi (✉ khorsandi.mostafa@gmail.com)

Institut national de la recherche scientifique <https://orcid.org/0000-0002-4359-1600>

Andre St-Hilaire

Institut national de la recherche scientifique

Richard Arsenault

École de technologie supérieure: Ecole de technologie superieure

Jean-Luc Martel

École de technologie supérieure: Ecole de technologie superieure

Samah Larabi

University of Victoria

Markus Schnorbus

University of Victoria

Francis Zwiers

University of Victoria

Research Article

Keywords: CEQUEAU model, Climate change, Nechako River, River temperature

Posted Date: August 30th, 2023

DOI: <https://doi.org/10.21203/rs.3.rs-2402073/v1>

License:  This work is licensed under a Creative Commons Attribution 4.0 International License.

[Read Full License](#)

1 **Future flow and water temperature scenarios in an impounded drainage basin:**
2 **Implications for summer flow and temperature management downstream of the dam**

3
4 **Abstract**

5 Water temperature is a key variable affecting fish habitat in rivers. The Sockeye salmon
6 (*Oncorhynchus nerka*), a keystone species in north western aquatic ecosystems of North
7 America, is profoundly affected by thermal regime changes in rivers, and it holds a pivotal role
8 in ecological and economic contexts due to its life history, extensive distribution and
9 commercial fishery. In this study, we explore the effects of climate change on the thermal
10 regime of the Nechako River (British Columbia, Canada), a relatively large river partially
11 controlled by the Skins Lake Spillway. The CEQUEAU hydrological-thermal model was
12 calibrated using discharge and water temperature observations. The model was forced using
13 the Fifth generation of ECMWF Atmospheric Reanalysis data for the past and meteorological
14 projections (downscaled and bias-corrected) from climate models for future scenarios.
15 Hydrological calibration was completed for the 1980-2019 period using data from two
16 hydrometric stations, and water temperature calibration was implemented using observations
17 for 2005-2019 from eight water temperature stations. Changes in water temperature were
18 assessed for two future periods (2040–2069 and 2070–2099) using eight Coupled Model
19 Intercomparison Project Phase 6 climate models and using two Shared Socioeconomic Pathway
20 scenarios (4.5 and 8.5 W/m² by 2100) for each period. Results show that water temperatures
21 above 20°C [an upper threshold for adequate thermal habitat for Sockeye salmon migration in
22 this river] at the Vanderhoof station will increase in daily frequency. While the frequency of
23 occurrence of this phenomenon is 1% (0-9 days/summer) based on 2005-2019 observations,
24 this number range is 3.8-36% (0-62 days/summer) according to the ensemble of climate change
25 scenarios. These results show the decreasing habitat availability for Sockeye salmon due to
26 climate change and the importance of water management in addressing this issue.

27 **Key Words**

28 CEQUEAU model, Climate change, Nechako River, River temperature

29 **1. Introduction**

30 The aquatic systems are threatened by natural and anthropogenic pressures, including land
31 cover change, flow regime change, and global climate change (Algera et al., 2022; Bosmans et
32 al., 2022). Of all these threats, climate change may have the most prolonged and largest-scale
33 impacts on various ecosystems, particularly in freshwater (Nash et al., 2017). Habitat loss
34 already has severe consequences for aquatic life like salmonids (Carrington, 2020), with a 76%
35 reduction in their global population and even more in some regions (93% in Europe) (Deinet
36 et al., 2020). It remains unclear how much of this habitat loss is due to climate change.
37 However, it has been shown that increased air temperature has changed North America's flow
38 regime and water temperatures (Islam et al., 2019). The river reaches located downstream of
39 dam facilities have managed flows, which can increase (via inadequate environmental flow
40 prescriptions) or reduce (through water releases) the impact of climate change (Ahmad et al.;
41 Algera et al., 2022; Fullerton et al., 2022; Sheedy, 2005; Sullivan and Rounds, 2021; Xiong et
42 al., 2019). There are multiple ways to mitigate the impact of climate change through man-made

43 efforts on the local scale. The analysis of dam operations as a potential mitigation method to
44 counteract climate change impacts on juvenile salmon was conducted by Sullivan and Rounds
45 (2021) and Stratton Garvin et al. (2022). They successfully utilized hydrodynamic models to
46 demonstrate that changes in dam operations, particularly at the upstream dam, can effectively
47 alter water temperatures released from the dam, with implications for seasonal temperature
48 patterns and downstream river temperature variations. Climate change affects juvenile salmon
49 through changes in water temperature, habitat availability, and food resources, influencing their
50 growth and survival. Dam operation simulations aimed to investigate scenarios that can
51 improve conditions for endangered anadromous fish by incorporating a temperature target.

52 A study conducted in the Nechako River watershed in Western Canada (Macdonald, 2019)
53 focused on assessing the approaches to alleviate the challenges posed by reservoir operation
54 and the resulting reduced water flows, both leading to unfavorable conditions for the Sockeye
55 salmon population. River water temperature plays a crucial role in aquatic life, and previous
56 studies have shown that temperature is one of the dominant factors influencing the Nechako
57 River watershed's aquatic habitats (Macdonald et al., 2007) because water temperature
58 significantly shapes the conditions essential for aquatic organisms' survival. It directly
59 influences the metabolic rates of aquatic organisms, affecting their growth, reproduction, and
60 overall physiological functions. Furthermore, temperature governs the solubility of gases in
61 water, impacting oxygen levels vital for aquatic species' survival (Macdonald, 2019). For
62 example, Islam et al. (2019) showed that summer water temperatures in the Fraser River
63 watershed, which includes the Nechako River as a sub-watershed, rose by 1°C during 1950-
64 2015. This rise in summer water temperature has doubled the number of days where the daily
65 average water temperature exceeded 20°C. Therefore, previous studies related to Sockeye
66 salmon (*Onchorhynchus Nerka*) habitat in the Nechako River resulted in a water temperature
67 management protocol during the summertime (Macdonald, 2019).

68 The Summer Temperature Management Program (STMP) water release protocol was
69 developed between 1980 and 1983 (Macdonald 2019) to mitigate water temperature increases
70 downstream of the Skins Lake Spillway (SLS), the hydraulic structure to control the river flow
71 downstream. Based on STMP, during the Sockeye salmon migration season, which lasts from
72 mid-July to mid-August, the SLS owner/manager (Rio Tinto, the mining company that owns
73 the Kenny Dam and SLS, also manages the water flow from SLS) releases volumes of water
74 to maintain average daily water temperatures below 20°C at Finmoore town, approximately 35
75 km upstream of the confluence of the Nechako and Stuart rivers. Moreover, understanding the
76 specific temperature ranges within which Sockeye salmon thrive is crucial. The known thermal
77 tolerances for Sockeye salmon (Middleton et al., 2018; Robinson et al., 2015) are summarized
78 in Table S1 in Online Resource (i.e., supplementary information, including detailed data in
79 tables and graphs).

80 In recent decades, multiple models have been used to assess the impacts of climate change on
81 river temperature, particularly on systems with salmonid populations around Canada (Ahmadi-
82 Nedushan et al., 2007; Dugdale et al., 2018; Kwak et al., 2017b; Wilson et al., 2015). Existing
83 water temperature models can be divided into three categories: (1) deterministic models
84 (Dugdale et al., 2017a), (2) classic statistical models (Benyahya et al., 2007), and (3) artificial
85 intelligence models as a subcategory of empirical models (Zhu and Piotrowski, 2020). Since
86 deterministic models explicitly formulate physical processes, they are often considered a

87 preferred tool for assessing possible shifts in water flow and temperature regimes under climate
88 change scenarios (Ouellet et al., 2020).

89 CEQUEAU, a hydrological-thermal model, is specifically designed for forecasting water
90 temperature at the watershed scale (Dugdale et al., 2017a; Ficklin et al., 2012). CEQUEAU is
91 a flexible modeling tool that allows adding new modules (e.g., options for different
92 evapotranspiration and snowmelt algorithms) (St-Hilaire et al., 2015), and the tool can be used
93 jointly with modern algorithms to achieve model calibration or to conduct a sensitivity analysis
94 (e.g., Khorsandi et al., 2022). CEQUEAU is also well-adapted for simulating dam release
95 operations and thermal modeling of rivers. For the Nechako River watershed, CEQUEAU has
96 been used for operational flow forecasting by Rio Tinto. Ouellet-Proulx et al. (2017a) studied
97 ensemble water temperature forecasting using water temperature and flow assimilation. The
98 model's source code for the evaporative heat loss module is improved (Ouellet-Proulx et al.,
99 2019). However, deterministic modeling using CEQUEAU is still needed to assess the
100 combined impact of flow regime change and climate change on the Nechako. Therefore, this
101 study attempts to provide guidance on this need by simulating the impacts of climate change
102 on the Nechako River in the context of STMP implementation with CEQUEAU. Therefore,
103 this study aims to:

- 104 - Calibrate the CEQUEAU model hydrologically and thermally using the multisite water
105 flow and temperature calibration method.
- 106 - Establish upstream boundary conditions by coupling CEQUEAU with other models
107 that simulate reservoir temperature and those found in tributaries emptying in the
108 reservoir (i.e., VIC-GL, RBO, and CE-QUAL-W2 models).
- 109 - Project future water temperatures using downscaled, bias-corrected meteorological
110 data, upstream models outputs as boundary conditions, and the calibrated CEQUEAU
111 model.
- 112 - Analyze these projected water temperatures, particularly focusing on compliance with
113 the mandatory 20°C threshold at the Vanderhoof station.

114 **2. Method**

115 **2.1. Study Area**

116 The Nechako River watershed is located in the central part of British Columbia, Canada, with
117 a 45,000 km² drainage area (Fig. 1). Downstream of Ootsa Lake (Fig. 1, the large lake
118 immediately upstream of SLS), the flow of the river is fully regulated by the SLS between the
119 Nechako Reservoir and its confluence with the Nautley River, after which the flows of the
120 Nechako and Nautley rivers combine and continue past the town of Vanderhoof and eventually
121 into the Fraser River. Three hydrometric stations measure the discharge (Environment and
122 Climate Change Canada, <https://www.canada.ca/en/environment-climate-change/>, data access:
123 May 2022). Those are at the SLS, the Nautley River (upstream of the confluence with the
124 Nechako River), and the town of Vanderhoof (see Fig. 1). The SLS flows and temperatures
125 provide the boundary conditions to the hydrological and thermal modules and are not used as
126 target stations for hydrological calibration. Eight stations measure water temperature (Rio
127 Tinto, data access: May 2022) in the watershed (Fig. 1). The study area and monitoring stations
128 are explained in detail in Ouellet-Proulx et al. (2017a) and Khorsandi et al. (2022).

129

[Fig. 1 Here]

2.2. CEQUEAU Model

CEQUEAU is a hydrological-thermal model designed explicitly for hydrological and surface water temperature modeling (Morin and Couillard, 1990; St-Hilaire et al., 2015). The model has been extensively tested in multiple case studies (Dugdale et al., 2018; Dugdale et al., 2017b; Fniguire et al., 2022; Kwak et al., 2017a; Kwak et al., 2017b; Ouellet-Proulx et al., 2017a; Ouellet-Proulx et al., 2017b).

Land cover and topography are required physiographic input data for the CEQUEAU model (Dugdale et al., 2017b). We used the most up-to-date global land cover data, with a 10 m spatial resolution provided by Environmental Systems Research Institute (ESRI) and the European Space Agency (ESA)(Karra et al., 2021; Zanaga et al., 2021). We used the National Aeronautics and Space Administration (NASA) SRTM Digital Elevation Model (SDEM) with 30 m spatial resolution (Farr et al., 2007) to calculate elevations in the CEQUEAU's input structure.

The CEQUEAU model conceptualizes a drainage basin as an interconnected network of hydrological response units called partial squares (CP; based on the French acronym in the CEQUEAU manual), delineated as sub-components of square grid cells (Fig. 2a). For each CP, the hydrological module calculates a simplified hydrological budget using a production function (PF) that simulates water routing into the surface runoff, interflow, and groundwater. Then a hydrological transfer function (TF) applies a routing scheme on the available surface water to calculate the water volume routed to the downstream CP (Fig. 2d). The PF uses precipitation and air temperature (minimum and maximum) as meteorological inputs (Fig. 2b). The hydrological module includes 26 global (i.e., one value for all CPs) parameters and then produces the output, i.e., simulated discharge (Fig. 2d).

[Fig. 2 Here]

2.3. Modeling Upstream Boundary Conditions

Flow and temperature at the SLS are the boundary conditions for the CEQUEAU model. These data are observed values at SLS (Environment and Climate Change Canada, <https://www.canada.ca/en/environment-climate-change/>, data access: May 2022) for the calibration period. In terms of temperature, one sensor is installed immediately downstream of SLS. The data for this sensor has been available since 2017. Therefore, for the calibration period, similar to previous studies on the Nechako using the CEQUEAU model (Ouellet-Proulx 2018, Ouellet-Proulx et al. 2017b, Ouellet-Proulx et al. 2017a), we calculated the average water temperature for each day of the year (DOY) using the observed data from 2017 to 2021.

A coupled hydrologic model simulates upstream boundary conditions for flow and temperature at SLS for future horizons (2040-2069 and 2070-2099): the Variable Infiltration Capacity (VIC-GL) (Liang et al., 1996, 1999; Schnorbus, 2018), the River Basin Model (RBM) (Larabi et al., 2022), the STMP reservoir operation program, and the CE-QUAL-W2 hydrodynamic

171 model (Cole and Wells, 2006) (Fig. 2). The coupled modeling platform aims to simulate the
172 governing processes of water flow and temperature feeding the reservoir and reservoir
173 hydrodynamics. The modeling platform allows for consideration of changes in timing and
174 volume of water availability to simulate reservoir thermal stratification and temperature of
175 water released at SLS.

176 The VIC-GL is an upgraded version of the VIC model, a spatially distributed land surface
177 model that accounts for glacier processes (Schnorbus, 2018). The VIC-GL model was
178 implemented at the upstream area of the Nechako Reservoir. The stream temperature model,
179 RBM, is a gridded physically-based model that uses a one-dimensional mixed Eulerian-
180 Lagrangian approach to simulate water temperature based on local air-water surface heat
181 exchange and advected heat flux from upstream. VIC-GL was coupled with RBM to simulate
182 discharge and water temperature at the main tributaries feeding the Nechako Reservoir (Larabi
183 et al., 2022). Both models were calibrated against observed discharge and water temperature at
184 the six main tributaries of the Nechako Reservoir as identified by Canada Water Survey
185 stations. They used input meteorological data for 1945-2018 at a 3-hour timestep for which
186 both observed water flow and water temperature data are available for different periods
187 depending on the station (Larabi et al., 2022). These models (VIC-GL, RBM, and CE-QUAL-
188 W2) did not need upstream conditions since each model provided upstream conditions for the
189 next one. Therefore, the calibration and validation were performed using partial time series
190 data availability and daily time steps for water flow and temperatures.

191 CE-QUAL-W2 is a mechanistic hydrodynamic model for water quality modeling (Cole and
192 Wells, 2006). This model uses a two-dimensional scheme to differentiate water bodies along
193 the river (longitudinal) and depth (vertical). This scheme makes this model suitable for
194 studying water flow and quality studies in large water bodies like dam reservoirs (Afshar et al.,
195 2011; Kim and Kim, 2006). The model assumes water is laterally well mixed but can be
196 vertically stratified. CE-QUAL-W2 can model water velocity and flow at different time scales
197 with the hydraulic sub-model. Also, these variables are input for the water quality sub-model,
198 which simulates temperature, dissolved oxygen, and multiple other variables required to study
199 aquatic life. The model requires meteorological data as well as boundary conditions of inflows
200 and outflows. Using VIC-GL and RBM to provide inflow boundary conditions and historical
201 powerhouse intake and water release at SLS, the CE-QUAL-W2 model was first calibrated
202 against historical reservoir water elevation for the period spanning 1986-2017. Then, the model
203 was calibrated against water temperature profiles at Kenney Dam (See Fig. 1, in the Nechako
204 River) and Natalkuz Lake (Upstream of Kenny Dam, Fig. 1) for the summer of 1994, as well
205 as outlet water temperature at SLS for the summer of 2016-2017 (See Fig. 1). The deployment
206 and calibration of the integrated modeling platform are discussed in detail by Larabi et al.
207 (2022).

208 Implementing the Summer Temperature Management Program (STMP) represents a crucial
209 facet of water flow regulation at the Nechako Reservoir (see Fig. 2c). As a response to the
210 significant influence of reservoir regulation on water quantity and quality in the Nechako River,
211 the STMP was introduced in 1983 with the primary objective of ameliorating conditions for
212 Sockeye salmon migration. The STMP focuses on mitigating elevated water temperatures
213 during the critical migration period from July 20 to August 20 at Finmoore. This program
214 involves augmenting water releases at the SLS during the migration period, effectively curbing
215 the frequency of water temperatures exceeding 20°C. The average water release is

216 approximately 32 m³/s at SLS during fall and winter to support Sockeye salmon. The water
217 release is increased during summer to a maximum limit (approximately 450 m³/s) in response
218 to warming trends. By orchestrating these controlled releases, the STMP plays a pivotal role in
219 preserving the ecological integrity of the Nechako River and sustaining the migratory patterns
220 of vital salmon species (Macdonald, 2019; Larabi et al., 2022).

221 To simulate future scenarios of temperatures and flows at SLS, the VIC-GL/RBM/CE-QUAL-
222 W2 combination of models is forced with future climate model outputs using two Shared
223 Socioeconomic Pathways (SSPs). These future hydrologic scenarios are then used as input to
224 the reservoir operation model (e.g., STMP) provided by Rio Tinto to simulate associated
225 scenarios of powerhouse intake and SLS discharge (Fig. 2b,c).

226 **2.4. Fifth Generation of ECMWF Atmospheric Reanalysis Data**

227 There is a need for complete meteorological data to calibrate and validate the hydrological
228 model for the historical period as the baseline to be compared with future scenarios. However,
229 there is no complete observed meteorological dataset for the basin in the past that can be used
230 as a reference dataset. Therefore, an alternative is to use climate reanalysis products, as Gatien
231 et al. (2022) suggested.

232 In addition to precipitation and air temperature, the CEQUEAU water temperature module
233 (Fig. 2d) requires wind speed, water vapor pressure, and net solar shortwave radiation. These
234 meteorological variables are provided by the European Center for Medium-Range Weather
235 Forecasting (ECMWF) through their European Reanalysis 5th generation (ERA5) (Hersbach et
236 al., 2020), with the exception of vapor pressure which was calculated using ERA5 dew point
237 temperature at 2 m height and with Teten's equation (Monteith and Unsworth, 2013; Murray,
238 1967). These gridded-based input data (with 30 × 30 km resolution) were interpolated to all
239 basin whole squares using the built-in CEQUEAU interpolator based on the nearest neighbors
240 approach (Ouellet-Proulx et al., 2019). ERA5 and climate models had three hours of temporal
241 time steps. After downscaling and bias correction for climate models, we converted these data
242 to daily time steps for running the CEQUEAU model.

243 **2.5. Model calibration and implementation**

244 This study uses multisite model calibration, using the maximum available information to
245 provide the best set of parameters for the whole watershed (Arsenault et al., 2018; Bérubé et
246 al., 2022; Shen et al., 2022). This study uses data from all available hydrometric (2) and water
247 temperature stations (8). First, the hydrological module with 26 parameters was calibrated
248 using the data from two hydrometric stations for June-September, which is the high-
249 temperature period of the year (Online Resource Table S2). Then, using the calibrated
250 hydrologic module outputs, the thermal module with eight parameters was calibrated using the
251 data from eight water temperature monitoring stations for the same period.

252 *2.5.1. Covariance Matrix Adaptation Evolution Strategy calibration algorithm*

253 This study uses the Covariance Matrix Adaptation Evolution Strategy (CMA-ES; Hansen and
254 Ostermeier, 1996) to find the optimal set of parameters for both hydrological and thermal
255 modules for CEQUEAU during model calibration. CMA-ES is an evolutionary algorithm
256 developed as a global optimization method (Hansen, 2016). This algorithm is frequently used
257 for hydrological model calibration (Elshall et al., 2015; Smaoui et al., 2018; Yu et al., 2012;

258 Zouhri et al., 2021). Arsenault et al. (2014) showed the superiority of CMA-ES in finding
 259 global optima and convergence speed compared to nine other well-known optimization
 260 algorithms used to calibrate hydrological models. Khorsandi et al. (2022) showed the efficiency
 261 of this method for thermal calibration of the CEQUEAU model for the Nechako watershed.
 262 This method can be summarized in four steps, which are explained in detail by Hansen (2016)
 263 and Khorsandi et al. (2022).

264 2.5.2. Hydrological Model Calibration

265 The objective function for the optimization algorithm is the Kling-Gupta Efficiency (KGE)
 266 (Gupta et al., 2009) coefficient, which is in Equations (1-5). The objective function in the
 267 calibration process shows the goodness of fit between simulated and observed data. Since every
 268 efficiency metric has its own strengths and limitations, presenting only one metric may be
 269 biased or may not accurately reflect the calibration's success. In addition to KGE, the Bias and
 270 Nash-Sutcliffe efficiency (NSE; Nash and Sutcliffe, 1970) metrics were also calculated as
 271 follows:

$$KGE_j = 1 - ED_j \quad (1)$$

$$ED_j = \sqrt{(r_j - 1)^2 + (\alpha_j - 1)^2 + (\beta_j - 1)^2} \quad (2)$$

$$r_j = \frac{\sum_{i=1}^N (O_{i,j} - \bar{O}_j) (S_{i,j} - \bar{S}_j)}{\sqrt{\sum_{i=1}^N (O_{i,j} - \bar{O}_j)^2} \sqrt{\sum_{i=1}^N (S_{i,j} - \bar{S}_j)^2}} \quad (3)$$

$$\alpha_j = \frac{\sigma_{S_j}}{\sigma_{O_j}} \quad (4)$$

$$\beta_j = \frac{\bar{S}_j}{\bar{O}_j} \quad (5)$$

$$Bias_j = \bar{O}_j - \bar{S}_j \quad (6)$$

$$NSE_j = 1 - \frac{\sum_{i=1}^N (S_{i,j} - O_{i,j})^2}{\sum_{i=1}^N (O_{i,j} - \bar{O}_j)^2} \quad (7)$$

272 where KGE_j , $Bias_j$ and NSE_j are the metrics for the j^{th} station; $O_{i,j}$ and $S_{i,j}$ respectively are
 273 observed and simulated values for the j^{th} station at the i^{th} time step; N is the number of time
 274 steps (measurements); r_j is the pearson correlation coefficient between observed and simulated
 275 values; α_j is the ratio of the standard deviation of simulated values to the standard deviation of
 276 observed values; β_j is the ratio of the mean of simulated values to the mean of observed values;
 277 σ_{S_j} and σ_{O_j} are the standard deviation of simulations and observations for the j^{th} station, and
 278 \bar{S}_j and \bar{O}_j are the mean of simulated and observed values. As previously recommended by
 279 Arsenault et al. (2018) and Shen et al. (2022), all the available data and stations were used for
 280 model calibration, which means that no data was reserved for validation.

281 2.5.3. Thermal Model Calibration

282 The eight thermal model parameters (Online Resource Table S3) - were adjusted using Root
283 Mean Square Error (RMSE) as the objective function and the CMA-ES algorithm for
284 optimization. The RMSE efficiency metric was used as recommended in the literature (Ouellet-
285 Proulx et al., 2017a; Ouellet-Proulx et al., 2019).

$$RMSE_j = \sqrt{\frac{\sum_{i=1}^N (S_{i,j} - O_{i,j})^2}{N}} \quad (8)$$

286 where $RMSE_j$ is the metric for the j^{th} station.

287 As with the hydrological calibration, all stations and all observed data were used for thermal
288 model calibration. Both hydrological and thermal calibrations were completed in a two-step
289 process. First, lower and upper boundaries for the model parameters were examined manually
290 to ensure that the simulations stayed within realistic limits when the parameter had a physical
291 meaning. Following this manual calibration, the CMA-ES optimization algorithm was used to
292 refine the model parameter values of the hydrological and thermal modules. These steps are
293 explained in detail by Khorsandi et al. (2022).

294 **2.6. Future Model Projections**

295 Following calibration, the calibrated CEQUEAU model was used to simulate water
296 temperature over the Nechako watershed for two future periods, 2040-2070 and 2070-2100,
297 using eight CMIP6's General Circulation Models (GCM) (Online Resource Table S4). The 4.5
298 and the 8.5 W/m² radiative forcing scenarios show the range of possible changes for the two
299 future periods compared to the baseline period (for 1980-2019, using the ERA5 dataset). We
300 selected the 4.5 and the 8.5 W/m² scenarios based on Shared Socioeconomic Pathways (SSP)
301 terminology agreed upon in CMIP6 (Online Resource Table S5), with 8.5 w/m² being the more
302 pessimistic scenario. . The water temperature simulations resulted in metrics for the river's
303 thermal regime. From all CMIP6 models, these eight models were selected to conduct this
304 study because they had all the required variables at sub-daily time steps. We used the sub-daily
305 time steps for bias correction, similar to Gatien et al. (Personal communication) for inter-model
306 comparison studies.

307 Each global climate model using SSP forcings provided all meteorological data to run the
308 model, which were bias-corrected using the N-dimensional Multivariate Bias Correction
309 algorithm (MBCn) algorithm (Cannon, 2018) with the ERA5 data as the reference dataset for
310 two radiative forcing scenarios (4.5 and 8.5 W/m²). Eight climate models were used, as
311 presented in Online Resource Table S4. The bias correction at the sub-daily timestep better
312 represents the meteorological data's diurnal cycle and improves the daily averages (Gatien et
313 al., 2022).

314 The MBCn algorithm is a novel approach in climatology that addresses limitations in
315 traditional bias correction methods. While many existing algorithms focus on univariate time
316 series and disregard the interdependencies between different variables, MBCn introduces a
317 multivariate perspective. Inspired by an image processing technique, it leverages the N-
318 dimensional probability density function transform to correct climate model projections of
319 multiple climate variables. MBCn generalizes quantile mapping, preserving the entire observed
320 continuous multivariate distribution in the corresponding climate model distribution. This

321 adapted technique accurately maintains the quantile changes between historical and projection
322 periods (Cannon, 2018).

323 Considering that the CEQUEAU model simulates water temperature at daily time steps, the
324 sub-daily variables were aggregated to generate daily meteorological time series (by averaging
325 for most variables and summing for precipitation). Finally, the daily meteorological projections
326 were forced into CEQUEAU, and the model simulated future discharge and water temperature
327 projections for the two periods mentioned above. Each GCM has a different gridded network,
328 which was interpolated for the CEQUEAU grid points using the nearest neighbors approach
329 (Ouellet-Proulx et al., 2019).

330 **2.7. Duration Curve Method**

331 All inputs and outputs for the CEQUEAU model have daily time steps in this study. For the
332 simulation outputs, temperature duration curves (TDC) were used to show and analyze the
333 daily water temperature simulations for the past and future periods. TDC plots the probability
334 of the exceedance of the observed value from multiple thresholds in a continuous manner
335 (Karakoyun et al., 2018). This study identified the probability of exceedance of the critical
336 environmental threshold of 20°C [an upper threshold for adequate thermal habitat for Sockeye
337 salmon migration in this river at Finmoore; Macdonald (2019)] on TDC curves. The TDC
338 curves in this study show the probability of exceedance for water temperatures higher than 5°C.
339 The temperatures above the 5°C threshold was selected because the CEQUEAU model is not
340 designed to model low (close to zero) water temperatures (e.g., there is no ice-formation
341 algorithm in CEQUEAU).

342 **3. Results**

343 **3.1. Hydrological module calibration and parameters**

344 Fig. 3 shows the simulated and observed discharge values for Vanderhoof and Nautley stations
345 during the calibration period.

346

347 [Fig. 3 Here]

348

349 Performance indicators were excellent for the Vanderhoof station (KGE = 0.94, NSE = 0.88)
350 (Fig. 3a), and the KGE value was acceptable for the Nautley station (KGE = 0.54, NSE = 0.4)
351 (Fig. 3b). Online Resource Table S2 shows the 26 calibrated hydrological parameters using the
352 multisite approach using these two observation stations. However, the simulated values at the
353 Nautley station show overestimations for high flows. This Bias for high flows is likely due to
354 the presence of two large lakes upstream of the station. The current version of the CEQUEAU
355 model conceptualizes the lake storage effect by using a single reservoir and a modified transfer
356 coefficient. However, a single calibrated value for CVMAR (Lakes and marshes drainage
357 coefficient in a CP) and HMAR (Lakes and marshes drainage threshold in a CP), the two
358 parameters associated with lake water storage, is likely not well-adapted to the lake cascade
359 configuration in the Nautley sub-watershed (See online resources Table S2). On the other hand,
360 for the Nautley station, high flows are not the priority in this study. As explained by Khorsandi
361 et al. (2022), high flows tend to occur in May and June, while the main focus of this research
362 is on the warm July-August period, for which the simulations for the Nautley station show

363 acceptable efficiency metrics ($KGE = 0.61$) with unbiased flow estimations ($Bias = 1.19\text{m}^3/\text{s}$,
364 relative Bias = 0.03).

365 **3.2. Thermal Model Calibration**

366 Online Resource Table S3 shows the thermal module parameter values using eight stations and
367 a multisite approach for calibration. The simulated time series versus observed values are
368 shown in Fig. 4 for eight stations using the calibrated values for thermal calibration.

369

370 [Fig. 4 Here]

371

372 For the stations with more extended observation periods and without water bodies upstream,
373 the CEQUEAU model can provide low Bias simulations with $RMSE < 2^\circ\text{C}$ and $Bias < 0.8^\circ\text{C}$
374 (Stations 1, 2, 3, 4, and 5). However, three of the eight stations (Stations 6, 7, and 8) show Bias
375 metrics higher than 1.5°C and RMSEs greater than 2°C . Again, this Bias is likely due to the
376 presence of large water bodies upstream of these stations. Large water bodies increase the
377 contact surface, which, during the summer period, has a warming effect on surface water
378 outflow. The current version of CEQUEAU does not consider this lake effect, which may
379 explain the underestimation of simulated water temperature. The impact of large lakes on the
380 CEQUEAU temperature simulations is further discussed by Khorsandi et al. (2022). The
381 Vanderhoof station (Station 2) is of higher importance because it is the closest station with
382 longest observation period to the location identified in the STMP (Finmoore), where the
383 average daily water temperature must remain $\leq 20^\circ\text{C}$ during the Sockeye salmon migration.

384 The simulated results for the Vanderhoof station for the baseline period show $RMSE = 1.27^\circ\text{C}$
385 and $Bias \approx 0^\circ\text{C}$, which are acceptable results when using a hydrological model at the watershed
386 scale. Although the simulated values are generally unbiased (Fig. 4), there is a slight
387 underestimation of the yearly number of days above 20°C (Fig. 5).

388 Fig. 5a shows that the average simulated temperatures matched the observed values for the
389 July-August period for each year. These simulated values use ERA5 data (one dataset) for the
390 1980-2019 baseline period, and each boxplot shows the simulated water temperature range in
391 a year. Fig. 5b shows the number of days above 20°C for both observed and simulated data.
392 Fig. 5b shows that the number of days above 20°C is not perfectly matched. Fig. 5b shows that
393 the error (observed - simulated) in the number of days above 20°C for simulated time series
394 ranges from -5 to +9 days. Hence, there are summers during which the model overestimates
395 the number of days above 20°C ; and there are summers during which the model underestimates
396 the number of days above 20°C . These differences in the simulated versus the observed number
397 of days should be considered when interpreting climate change simulations. The observed data
398 show that the maximum number of days above 20°C that occurred in a year is nine days (during
399 the July-August of 2019 in Fig. 5b). Simulations indicate that the highest historical number of
400 exceedances of 20°C is nine days (2016; Fig. 5b). The STMP aims to regulate elevated water
401 temperatures during sockeye salmon migration in the Nechako River by manipulating the
402 timing and volume of reservoir water releases from SLS (Bond, 2017). The management plan
403 focuses on maintaining average daily water temperatures at or below 20°C in the Nechako
404 River at Finmoore (30 km downstream of Vanderhoof), upstream of the Stuart River
405 confluence, during the critical migration period from July 20 to August 20. Cooler water

406 temperatures are essential for the survival of Sockeye salmon during its migration. The
407 program employs a comprehensive approach involving field data collection, weather forecasts,
408 temperature predictions, and flow release decisions. By analyzing trends in observed and
409 predicted water temperatures, Rio Tinto determines when to increase or decrease the release of
410 water from SLS, aiming to achieve optimal conditions for salmon migration. This protocol
411 enhances the resilience of the Nechako River ecosystem and contributes to the conservation of
412 Sockeye salmon populations. The program also employs a decision protocol to adjust SLS
413 releases between 14.2-453 m³/s based on observed and forecasted water temperature trends,
414 ensuring that the water temperature remains below the critical threshold for salmon survival.
415 Additionally, the release of water from SLS is carefully managed to maintain flow below
416 Cheslatta Falls (Fig. 1) between 170 m³/s and 283 m³/s.

417

418 [Fig. 5 Here]

419

420 Fig. 6a compares TDC for observations with simulated values (for values greater than 5°C).
421 Fig. 6a shows the probability of exceedance for water temperatures higher than the 5°C since
422 the CEQUEAU model is not designed to model low water temperatures. Fig. 6b shows the
423 timing of interannual averaged values for each DOY from 1980 to 2019 for observed and
424 simulated values during the warm months (from June to September). Fig. 6b shows that the
425 simulated values mostly follow the same timing pattern as the observed values. Although
426 simulated temperatures lag a few days behind observed ones, the observed values fall within
427 the lower and upper boundaries of simulated water temperatures. Fig. 6b also shows that in
428 long-term management through STMP implementation (adjusting SLS releases between 14.2-
429 453 m³/s at SLS from July 20 to August 20), STMP decreases the water temperature at the
430 Vanderhoof and the DOY average during the warm season is below the 20°C threshold, as
431 confirmed by observed water temperature values.

432

433 [Fig. 6 Here]

434

435 Fig. 4 (for the Vanderhoof station in higher resolution, see Fig. S1 in Online Resource) shows
436 that for Vanderhoof Station on a short-term daily basis, the CEQUEAU model can accurately
437 reproduce high-temperature days. Fig. 6b shows this ability in the long term over the years
438 through DOY averaged values. Therefore, the CEQUEAU simulated values for future climate
439 change scenarios can provide reliable insight into the timing and extent of changes in high
440 water temperatures.

441 3.3. Future projections

442 The selected climate scenarios data were used as inputs to the CEQUEAU model (Fig. 2b). In
443 addition, simulated water flow and water temperature at the SLS using CE-QUAL-W2 were
444 used as boundary conditions for the CEQUEAU model for future scenarios. Figures S2-S5 in
445 Online Resource show the simulated temperature results for the Vanderhoof station for the

446 SSP2-4.5 2040-2069, SSP2-4.5 2070-2099, SSP5-8.5 2040-2069, and SSP5-8.5 2070-2099
447 horizons, respectively.

448 Fig. 7 for the Vanderhoof station shows an increase in summer water temperature compared to
449 the baseline period (Fig. 6a). Fig. 6a shows TDC for the baseline, while Fig. 7 provides TDC
450 at the Vanderhoof station for all climate change scenarios. Figures S2-S5 in Online Resource
451 also show this increase in water temperature for future horizons compared to the baseline (Fig.
452 4 and Fig. S1 in Online Resource) for daily simulations. The range of the yearly increase range
453 can be seen in Online Resource Figures S6-S9.

454 Fig. 7 shows TDC for all eight climate models for all four climate change scenarios. As
455 expected, these scenarios show a higher probability of exceedance for 20°C compared to the
456 baseline period. The increasing probability of occurrence can be seen by moving from SSP4.5
457 to SSP8.5 and by going further in the time horizon. The exceedance probability starts from
458 3.8% for SSP2-4.5 (2040-2069 horizon) as the lowest value using MPI-ESM1-2-HR model
459 data, and the highest exceedance value is 36% for SSP5-8.5 (2070-2099 horizon) using CMCC-
460 ESM2 model data.

461

[Fig. 7 Here]

463

464 Fig. 8 shows the change in the timing of high temperatures for future time horizons. When
465 compared to Fig. 6b, it can be seen that August remains the warmest month, but September is
466 warming more than July. Fig. 6b indicates that the crucial time of year for warming is mid-July
467 to mid-August, which corresponds to the STMP period. This crucial warming period will
468 become longer and warmer in the future. The future warm summers are expected to start in
469 early July and last until early September. Considering the STMP fixed period (July 20 to
470 August 20), we calculate the onset and end temperature for STMP using the interannual average
471 data for the baseline period. This onset-end threshold equals 17°C (by using Fig. 6b for July
472 20 to August 20 period). Fig. 8 shows future scenarios for which June 8 to June 27 is the range
473 for the future 17°C onset and September 12 to 25 is the end of the 17°C threshold (Table 1),
474 which means more prolonged periods of warm days above these thresholds.

475

[Table 1 Here]

476

[Fig. 8 Here]

477

478

479 Fig. 9 shows the mean and median temperature for the July-August period on a yearly basis,
480 along with the number of days above 20°C per year. This figure provides a better understanding
481 of the potential frequency and duration of thermally stressful events for Sockeye salmon in
482 future scenarios compared to the past (shown in Fig. 5).

483

[Fig. 9 Here]

484

485

486 The number of days above 20°C during summer each year differs between the four situations.
487 Figures S6-S9 in Online Resource show this variability among models. The four situations
488 (SSP4.5 and SSP8.5 for the 2040-2069 and 2070-2099 periods) show an increasing maximum
489 number of days above 20°C during summer, ranging from 38 to 62 days, which is above the
490 model uncertainty of nine days for this criterion. The SSP8.5 for the 2070-2099 period shows
491 that the daily average water temperature for the STMP period is above 20°C. Future water
492 temperature scenarios consistently show higher annual numbers of threshold exceedances than
493 the maximum level that occurred during the baseline period, which was nine days.

494 **4. Discussion**

495 **4.1. Hydrothermal modeling**

496 The CEQUEAU calibration metrics are satisfactory (KGE and $NSE \geq 0.6$), comparable or
497 better than those provided in previous studies on the Nechako (Online Resource Table S6)
498 (Islam et al., 2019; Kwak et al., 2017b; Ouellet-Proulx, 2018; Ouellet-Proulx et al., 2017b;
499 Ouellet-Proulx et al., 2019). Even though simulated flows and temperatures are comparable to
500 or better than in previous studies on Nechako (Ouellet-Proulx et al., 2017b; Ouellet-Proulx et
501 al., 2019; Ouellet et al., 2020), the hydrological calibration for the Nautley station shows
502 weaker performance metrics than at Vanderhoof. It is suspected that the weaker model
503 performance at this station is related to the impact of relatively large lakes upstream of the
504 station. The CEQUEAU model can conceptually account for the slower water routing through
505 lakes, but it is somewhat limited since it considers flow routing in a simplified and conceptual
506 form. Given that little is known about the water residence time in those lentic habitats, this
507 could be revisited if additional information is gathered. Khorsandi et al. (2022) also showed
508 that simulated water temperature is positively biased downstream of large water bodies in the
509 Nechako River watershed (e.g., the CEQUEAU simulations are underestimating the observed
510 temperature values downstream of the large water bodies). Lake surfaces provide a large area
511 exposed to solar radiation, leading to warming surface water. Stations 6-8 in Fig. 4 show this
512 Bias (underestimation in water temperature) for the stations upstream of the Nautley
513 confluence. However, this Bias does not spread downstream since the water temperature is
514 mainly controlled by local meteorological forcings (Khorsandi et al., 2022; Gatien et al., 2022).
515 As a result, the simulations at the Vanderhoof station are unbiased. Therefore, we can say the
516 future projections at the Vanderhoof station are unbiased too.

517 For stations 6-8, part of this Bias may be due to water temperature boundary conditions at SLS.
518 Synthetic time series were produced using DOY averages for the reference period. Gatien et
519 al. (2022), using the HEC-RAS hydraulic model for the reaches of the Nechako River between
520 the SLS and Vanderhoof, showed that the impact of upstream boundary conditions on the
521 simulated temperature at Vanderhoof is insignificant. Khorsandi et al. (2022) also showed that
522 local meteorological variables have a more significant impact than upstream conditions in the
523 Nechako, especially at Vanderhoof. However, since CEQUEAU does not include a complex
524 hydraulic water routing scheme like HEC-RAS, upstream boundary conditions may impact the
525 stations upstream of the Nautley confluence (Stations 6-8), which may partly explain the
526 presence of thermal simulation biases.

527 **4.2. Future Upstream Boundary Conditions Impacts on Downstream Water**
528 **Temperature**

529 This study used the CE-QUAL-W2 outputs for water temperature at the SLS based on using
530 current reservoir operations (STMP) to constrain the upstream boundary condition. The current
531 reservoir operation model defines powerhouse water intake and SLS outputs. This assumption
532 is based on a business-as-usual operation based on STMP by Rio Tinto and considers the water
533 temperature stratification inside the reservoir due to climate change impacts. Although CE-
534 QUAL-W2 resolves water stratification inside the reservoir, water is only released at SLS from
535 the surface layer of the reservoir, and reservoir management cannot provide cold water to the
536 Nechako River unless the water is taken from deeper layers. However, both flow and
537 temperature may experience regime shifts due to the impact of climate change on reservoir
538 stratification and climate change mitigations by Rio Tinto (e.g., future updated STMP or
539 installing a new water release facility). Currently, there is no facility to manage water
540 temperature downstream at the Nechako Reservoir directly. Therefore, testing other reservoir
541 management rules that explicitly consider water temperature downstream to reduce the
542 exceedance of the 20°C threshold is required. Further studies can analyze the implications and
543 efficiency of these changes on the upstream boundary conditions under climate change
544 scenarios.

545 **4.3. Future Water Temperature Simulation under Climate Change Impacts**

546 The results emphasize a projected increase in water temperature at the Vanderhoof station
547 during the 2040 to 2100 period. Past observed water temperature data and historical simulations
548 at Vanderhoof show similar exceedances of the 20°C threshold (1% for observations and
549 simulations; observations exist from 2005-2019). Islam et al. (2019) modeled temperatures for
550 the 1950-2015 historical period and found that the number of days above 20°C in the
551 summertime doubled over 65 years for the whole basin, and the whole Fraser River basin's
552 average summer temperature rose by 1°C during this period.

553 They reported that during the summer periods of 1960 to 2000 there was a three days decrease
554 in 20°C exceedances for the Vanderhoof station. This small reduction in 20°C exceedances for
555 Vanderhoof station while reporting warmer water at the Fraser basin may be explained by the
556 implementation of the STMP protocol by Rio Tinto, which focused on the Vanderhoof station
557 to keep the average temperature below the 20°C threshold.

558 Picketts et al. (2017) reported an increasing trend in water temperature for the Nechako
559 watershed during summertime using climate change impact assessments. Warmer summers
560 mean limiting conditions for Sockeye salmon, their migration, and spawning time upstream of
561 Vanderhoof station (Macdonald, 2019). Our simulations for exceedance of 20°C in near
562 climate horizons (2040-2069) show 0-36 days for SSP 4.5 and 0-58 days for SSP 8.5, which is
563 a significant increase. Picketts et al. (2017) mentioned a water temperature increase of around
564 2°C for this horizon using regional studies. Results for far future horizons (2070-2099) show
565 even higher exceedance frequencies for the 20°C threshold. Our estimations indicate 3-62 days
566 for SSP2-4.5. The SSP5-8.5 scenario simulations show 53-62 days beyond the 20°C threshold.
567 These simulations resulted from considering natural or at least historic flow rules based on
568 STMP. However, it may be possible to modify SLS water releases to target longer and more
569 frequent heat waves to mitigate the increase in temperatures.

570 **4.4. Ecological Implications of Nechako River Water Temperature Warming**

571 Sockeye salmon is one of the most vulnerable species to rising water temperatures, with 100%
572 mortality beyond 21°C in water temperature after 72 hours following exhaustive exercise
573 (Middleton et al., 2018; Robinson et al., 2015). Scatter plots of the daily average temperature
574 from July-August for each year of the baseline period (Fig. 5) indicate some years with nine
575 days above 20°C, with a rising trend in the number of days.

576 All four projections (SSP2-4.5 and SSP5-8.5 for 2040-2069 and 2070-2099) show an
577 increasing water temperature and an increased frequency of days with > 20°C water
578 temperature. While for the past period, the maximum number of exceedance days is 9 for each
579 summer, for these four combinations, the maximum number of 36, 62, 58, and 62 days is
580 expected based on daily simulations using eight climate models. Considering the lethal
581 threshold for Sockeye salmon (Online Resource Table S1), the number of days with a
582 temperature of more than 20°C is a severe and alarming signal for this species' habitat
583 (Carrington, 2020).

584 **4. Conclusion**

585 This study provided water temperature simulations for the historical baseline period of 1980-
586 2019, for the near future (2040-2069), and far future (2070-2099) for the Nechako River in
587 British Columbia, Canada. The study used CMIP6 climate models and SSP2-4.5 and SSP5-8.5
588 climate change scenarios. The CEQUEAU model was forced with ERA5 data for the past and
589 eight CMIP6 climate models for the future. The study's main finding was the ability of the
590 model to accurately simulate water temperatures during the summer at all eight observation
591 sites. The CEQUEAU model provided reliable water flow and temperature values for the entire
592 Nechako River watershed. The results of the study provide ensemble estimations of water
593 temperature under climate change scenarios, which are necessary for decision-makers in the
594 Nechako River watershed. Climate change scenarios indicate that there will be 3.8-36% more
595 days with water temperatures higher than 20°C, which may pose a severe threat to the Sockeye
596 salmon population due to changes in the Nechako River's thermal regime. The frequency of
597 days with an average water temperature of more than 20°C is expected to be 0-62 days during
598 July-August, compared to 0-9 days in the past. The water temperature simulation results
599 indicated a relatively high probability of exceeding the 20°C thermal limit at Vanderhoof in
600 the Nechako River. Scenarios indicate that potentially highly stressful conditions for cold-
601 water species like Sockeye salmon during high-temperature events will likely occur more
602 frequently. Future studies are needed to assess the possible impact of dam operation as an
603 adaptation strategy to tackle this and to implement other solutions as mitigation for increasing
604 water temperature.

605

606 **Statements & Declarations**

607 **Funding**

608 This work was funded by the Canadian Natural Sciences and Engineering Research Council
609 (NSERC) and Rio Tinto as part of a Collaborative Research and Development grant (Grant
610 Number: CRDPJ 523640-18).

611

612 **Competing Interests**

613 The authors have no relevant financial or non-financial interests to disclose.

614

615 **Data Availability**

616 Data will be made available on request.

617

618 **Acknowledgment**

619 The authors would like to thank the anonymous reviewers for their insightful and constructive
620 comments that helped us substantially improve the quality of our study.

621 **References**

622 Afshar A, Kazemi H, Saadatpour M (2011) Particle swarm optimization for automatic calibration of
623 large scale water quality model (CE-QUAL-W2): Application to Karkheh Reservoir, Iran. *Water
624 resources management* 25:2613-2632.

625 Ahmad SK, Hossain F, Holtgrieve GW, Pavelsky T, Galelli S Predicting the likely thermal impact of
626 current and future dams around the world. *Earth's Future* n/a:e2020EF001916.

627 Ahmadi-Nedushan B, St-Hilaire A, Ouarda TB, Bilodeau L, Robichaud E, Thiémonge N, Bobée B
628 (2007) Predicting river water temperatures using stochastic models: case study of the Moisie River
629 (Québec, Canada). *Hydrological Processes: An International Journal* 21:21-34.

630 Algera DA, Kamal R, Ward TD, Pleizier NK, Brauner CJ, Crossman JA, Leake A, Zhu DZ, Power M,
631 Cooke SJ (2022) Exposure risk of fish downstream of a hydropower facility to supersaturated total
632 dissolved gas. *Water Resources Research* n/a:e2021WR031887.

633 Arsenault R, Brissette F, Martel J-L (2018) The hazards of split-sample validation in hydrological
634 model calibration. *Journal of hydrology* 566:346-362.

635 Arsenault R, Poulin A, Côté P, Brissette F (2014) Comparison of stochastic optimization algorithms in
636 hydrological model calibration. *Journal of Hydrologic Engineering* 19:1374-1384.

637 Benyahya L, Caissie D, St-Hilaire A, Ouarda TB, Bobée B (2007) A review of statistical water
638 temperature models. *Canadian Water Resources Journal* 32:179-192.

639 Bérubé S, Brissette F, Arsenault R (2022) Optimal Hydrological Model Calibration Strategy for Climate
640 Change Impact Studies. *Journal of Hydrologic Engineering* 27:04021053.

641 Bond J (2017) 2017 Summer water temperature and flow management project. Triton Environmental
642 Consultants Ltd., BC, Canada, p. 40.

643 Bosmans J, Wanders N, Bierkens MFP, Huijbregts MAJ, Schipper AM, Barbarossa V (2022)
644 FutureStreams, a global dataset of future streamflow and water temperature. *Scientific Data* 9:307.

645 Cannon AJ (2018) Multivariate quantile mapping bias correction: an N-dimensional probability density
646 function transform for climate model simulations of multiple variables. *Climate Dynamics* 50:31-49.

647 Carrington D (2020) Migratory river fish populations plunge 76% in past 50 years. *The Guardian*. *The
648 Guardian*.

649 Cole TM, Wells SA (2006) CE-QUAL-W2: A two-dimensional, laterally averaged, hydrodynamic and
650 water quality model, version 3.5.

651 Deinet S, Scott-Gatty K, Rotton H, Twardek WM, Marconi V, McRae L, Baumgartner LJ, Brink K,
652 Claussen JE, Cooke SJ (2020) The living planet index (LPI) for migratory freshwater fish: Technical
653 report.

654 Dugdale SJ, Allen Curry R, St-Hilaire A, Andrews SN (2018) Impact of Future Climate Change on
655 Water Temperature and Thermal Habitat for Keystone Fishes in the Lower Saint John River, Canada.
656 *Water Resources Management* 32:4853-4878.

657 Dugdale SJ, Hannah DM, Malcolm IA (2017a) River temperature modelling: A review of process-
658 based approaches and future directions. *Earth-Science Reviews* 175:97-113.

659 Dugdale SJ, St-Hilaire A, Allen Curry R (2017b) Automating drainage direction and physiographic
660 inputs to the CEQUEAU hydrological model: sensitivity testing on the lower Saint John River
661 watershed, Canada. *Journal of Hydroinformatics* 19:469-492.

662 Elshall AS, Pham HV, Tsai FT-C, Yan L, Ye M (2015) Parallel inverse modeling and uncertainty
663 quantification for computationally demanding groundwater-flow models using covariance matrix
664 adaptation. *Journal of Hydrologic Engineering* 20:04014087.

665 Farr TG, Rosen PA, Caro E, Crippen R, Duren R, Hensley S, Kobrick M, Paller M, Rodriguez E, Roth
666 L, Seal D, Shaffer S, Shimada J, Umland J, Werner M, Oskin M, Burbank D, Alsdorf D (2007) The
667 Shuttle Radar Topography Mission. *Reviews of Geophysics* 45.

668 Ficklin DL, Luo Y, Stewart IT, Maurer EP (2012) Development and application of a
669 hydroclimatological stream temperature model within the Soil and Water Assessment Tool. *Water
670 Resources Research* 48.

671 Fnguire F, Laftouhi N-E, Al-Mahfadi AS, El Himer H, Khalil N, Saidi ME (2022) Hydrological
672 modelling using the distributed hydrological model CEQUEAU in a semi-arid mountainous area: a case
673 study of Ourika watershed, Marrakech Atlas, Morocco. *Euro-Mediterranean Journal for Environmental
674 Integration*.

675 Fullerton AH, Sun N, Baerwalde MJ, Hawkins BL, Yan H (2022) Mechanistic Simulations Suggest
676 Riparian Restoration Can Partly Counteract Climate Impacts to Juvenile Salmon. *JAWRA Journal of
677 the American Water Resources Association* n/a.

678 Gatien P, Arsenault R, Martel J-L, St-Hilaire A (2022) Using the ERA5 and ERA5-Land reanalysis
679 datasets for river water temperature modelling in a data-scarce region.

680 Gupta HV, Kling H, Yilmaz KK, Martinez GF (2009) Decomposition of the mean squared error and
681 NSE performance criteria: Implications for improving hydrological modelling. *Journal of hydrology
682* 377:80-91.

683 Hansen N (2016) The CMA evolution strategy: A tutorial. arXiv preprint arXiv:1604.00772.

684 Hersbach H, Bell B, Berrisford P, Hirahara S, Horányi A, Muñoz-Sabater J, Nicolas J, Peubey C, Radu
685 R, Schepers D, Simmons A, Soci C, Abdalla S, Abellan X, Balsamo G, Bechtold P, Biavati G, Bidlot
686 J, Bonavita M, De Chiara G, Dahlgren P, Dee D, Diamantakis M, Dragani R, Flemming J, Forbes R,
687 Fuentes M, Geer A, Haimberger L, Healy S, Hogan RJ, Hólm E, Janisková M, Keeley S, Laloyaux P,
688 Lopez P, Lupu C, Radnoti G, de Rosnay P, Rozum I, Vamborg F, Villaume S, Thépaut J-N (2020) The
689 ERA5 global reanalysis. *Quarterly Journal of the Royal Meteorological Society* 146:1999-2049.

690 Islam SU, Hay RW, Déry SJ, Booth BP (2019) Modelling the impacts of climate change on riverine
691 thermal regimes in western Canada's largest Pacific watershed. *Scientific Reports* 9:11398.

692 Karakoyun Y, Yumurtacı Z, Dönmez AH (2018) Chapter 4.9 - Environmental Flow Assessment
693 Methods: A Case Study. in Dincer I, Colpan CO, Kizilkan O (eds.) *Exergetic, Energetic and
694 Environmental Dimensions*. Academic Press, pp. 1061-1074.

695 Karra K, Kontgis C, Statman-Weil Z, Mazzariello JC, Mathis M, Brumby SP Global land use/land cover
696 with Sentinel 2 and deep learning. in 2021 IEEE International Geoscience and Remote Sensing
697 Symposium IGARSS, IEEE, Brussels, Belgium, pp. 4704-4707.

698 Khorsandi M, St-Hilaire A, Arsenault R (2022) Multisite calibration of a semi-distributed hydrologic
699 and thermal model in a large Canadian watershed. *Hydrological Sciences Journal*.

700 Kim Y, Kim B (2006) Application of a 2-dimensional water quality model (CE-QUAL-W2) to the
701 turbidity interflow in a deep reservoir (Lake Soyang, Korea). *Lake and Reservoir Management* 22:213-
702 222.

703 Kwak J, St-Hilaire A, Chebana F (2017a) A comparative study for water temperature modelling in a
704 small basin, the Fourchue River, Quebec, Canada. *Hydrological Sciences Journal* 62:64-75.

705 Kwak J, St-Hilaire A, Chebana F, Kim G (2017b) Summer season water temperature modeling under
706 the climate change: Case study for fourchue river, Quebec, Canada. *Water (Switzerland)* 9.

707 Larabi S, Schnorbus MA, Zwiers F (2022) A coupled streamflow and water temperature (VIC-RBM-
708 CE-QUAL-W2) model for the Nechako Reservoir. *Journal of Hydrology: Regional Studies* 44:101237.

709 Liang X, Wood EF, Lettenmaier DP (1996) Surface soil moisture parameterization of the VIC-2L
710 model: Evaluation and modification. *Global and Planetary Change* 13:195-206.

711 Liang X, Wood EF, Lettenmaier DP (1999) Modeling ground heat flux in land surface parameterization
712 schemes. *Journal of Geophysical Research: Atmospheres* 104:9581-9600.

713 Macdonald J (2019) Expert report for The Department of Justice.

714 Macdonald J, Morrison J, Patterson D, Heinonen J, Foreman M (2007) Examination of factors
715 influencing Nechako River discharge, temperature, and aquatic habitats. *Canadian Technical Report of*
716 *Fisheries and Aquatic Sciences* 2773:32.

717 Middleton CT, Hinch SG, Martins EG, Braun DC, Patterson DA, Burnett NJ, Minke-Martin V,
718 Casselman MT (2018) Effects of natal water concentration and temperature on the behaviour of up-
719 river migrating sockeye salmon. *Canadian Journal of Fisheries and Aquatic Sciences* 75:2375-2389.

720 Monteith J, Unsworth M (2013) *Principles of environmental physics: plants, animals, and the*
721 *atmosphere*. Academic Press.

722 Morin G, Couillard D (1990) Predicting river temperatures with a hydrological model. Chapter 5.
723 *Encyclopedia of Fluid Mechanics: Surface and Groundwater Flow Phenomena*. Volk Gulf Publishing
724 Company, Houston, Tex.

725 Murray FW (1967) On the Computation of Saturation Vapor Pressure. *Journal of Applied Meteorology*
726 *and Climatology* 6:203-204.

727 Nash JE, Sutcliffe JV (1970) River flow forecasting through conceptual models part I—A discussion
728 of principles. *Journal of hydrology* 10:282-290.

729 Nash KL, Cvitanovic C, Fulton EA, Halpern BS, Milner-Gulland EJ, Watson RA, Blanchard JL (2017)
730 Planetary boundaries for a blue planet. *Nature Ecology & Evolution* 1:1625-1634.

731 Ouellet-Proulx S (2018) *Prévision thermique d'ensemble en rivière avec assimilation de données*,
732 *Université du Québec, Institut national de la recherche scientifique*.

733 Ouellet-Proulx S, Chiadjeu OC, Boucher M-A, St-Hilaire A (2017a) Assimilation of water temperature
734 and discharge data for ensemble water temperature forecasting. *Journal of hydrology* 554:342-359.

735 Ouellet-Proulx S, St-Hilaire A, Boucher M-A (2017b) Water temperature ensemble forecasts:
736 Implementation using the CEQUEAU model on two contrasted river systems. *Water* 9:457.

737 Ouellet-Proulx S, St-Hilaire A, Boucher MA (2019) Implication of evaporative loss estimation methods
738 in discharge and water temperature modelling in cool temperate climates. *Hydrological Processes*.

739 Ouellet V, St-Hilaire A, Dugdale SJ, Hannah DM, Krause S, Proulx-Ouellet S (2020) River temperature
740 research and practice: Recent challenges and emerging opportunities for managing thermal habitat
741 conditions in stream ecosystems. *Science of The Total Environment* 736:139679.

742 Picketts IM, Parkes MW, Déry SJ (2017) Climate change and resource development impacts in
743 watersheds: Insights from the Nechako River Basin, Canada. *The Canadian Geographer / Le Géographe*
744 *canadien* 61:196-211.

745 Robinson KA, Hinch SG, Raby GD, Donaldson MR, Robichaud D, Patterson DA, Cooke SJ (2015)
746 Influence of postcapture ventilation assistance on migration success of adult sockeye salmon following
747 capture and release. *Transactions of the American Fisheries Society* 144:693-704.

748 Schnorbus M (2018) VIC Glacier (VIC-GL)-Description of VIC model changes and upgrades. VIC
749 Generation.

750 Sheedy B (2005) Analysis of a cold water release facility in the Nechako Reservoir, Faculty of Business
751 Administration-Simon Fraser University.

752 Shen H, Tolson BA, Mai J (2022) Time to Update the Split-Sample Approach in Hydrological Model
753 Calibration. *Water Resources Research* 58:e2021WR031523.

754 Smaoui H, Zouhri L, Kaidi S, Carlier E (2018) Combination of FEM and CMA-ES algorithm for
755 transmissivity identification in aquifer systems. *Hydrological Processes* 32:264-277.

756 St-Hilaire A, Boucher M-A, Chebana F, Ouellet-Proulx S, Zhou QX, Larabi S, Dugdale S, Latraverse
757 M Breathing a new life to an older model: The CEQUEAU tool for flow and water temperature

758 simulations and forecasting. in Proceedings of the 22nd Canadian Hydrotechnical Conference,
759 Montreal, QC, Canada.

760 Stratton Garvin LE, Rounds SA, Buccola NL (2022) Updates to models of streamflow and water
761 temperature for 2011, 2015, and 2016 in rivers of the Willamette River Basin, Oregon. Open-File
762 Report, Reston, VA.

763 Sullivan AB, Rounds SA (2021) Modeling water temperature response to dam operations and water
764 management in Green Peter and Foster Lakes and the South Santiam River, Oregon. Scientific
765 Investigations Report, Reston, VA.

766 Wilson KL, Kay LM, Schmidt AL, Lotze HK (2015) Effects of increasing water temperatures on
767 survival and growth of ecologically and economically important seaweeds in Atlantic Canada:
768 implications for climate change. *Marine Biology* 162:2431-2444.

769 Xiong Y, Yin J, Zhao S, Qiu GY, Liu Z (2019) How the Three Gorges Dam affects the hydrological
770 cycle in the mid-lower Yangtze River: a perspective based on decadal water temperature changes.
771 *Environmental Research Letters*.

772 Yu X, Bhatt G, Duffy C, Shi Y A Two-Scale Parameterization for Distributed Watershed Modeling
773 Using National Data and Evolutionary Algorithm. in AGU Fall Meeting Abstracts, pp. H31H-1231.

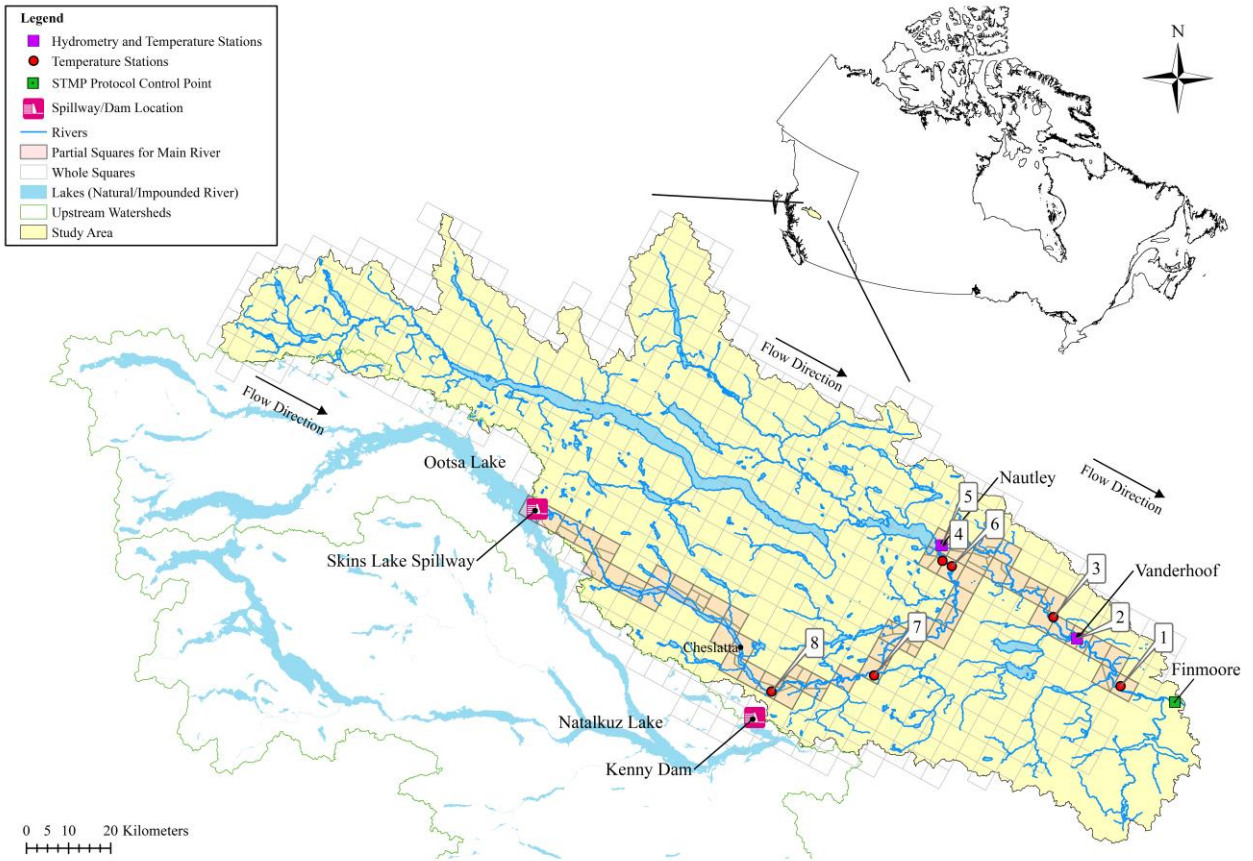
774 Zanaga D, Van De Kerchove R, De Keersmaecker W, Souverijns N, Brockmann C, Quast R, Wevers
775 J, Grosu A, Paccini A, Vergnaud S, Cartus O, Santoro M, Fritz S, Georgieva I, Lesiv M, Carter S,
776 Herold M, Li L, Tsendbazar N-E, Ramoino F, Arino O (2021) ESA WorldCover 10 m 2020 v100.

777 Zhu S, Piotrowski AP (2020) River/stream water temperature forecasting using artificial intelligence
778 models: a systematic review. *Acta Geophysica*:1-10.

779 Zouhri L, Kaidi S, Smaoui H (2021) Parameter Identification by High-Resolution Inverse Numerical
780 Model Based on LBM/CMA-ES: Application to Chalk Aquifer (North of France). *Water* 13:1574.

781 **Table 1** The onset and end dates for the 17°C thermal threshold (Fig. 6b) based on the STMP
782 period (July 20 to August 20)

Scenario	Onset date (for 17°C)	End date (for 17°C)	Duration (days)
Baseline-ERA5, 1980-2019	July 20	August 20	32
SSP2-4.5, 2040-2069	June 27	September 12	78
SSP2-4.5, 2070-2099	June 16	September 14	91
SSP5-8.5, 2040-2069	June 16	September 16	93
SSP5-8.5, 2070-2099	June 8	September 25	110



784

785

786

787

788

789

790

791

792

793

Fig. 1 Nechako River watershed study area. The hydrometry/temperature stations are numbered 1 to 8 from downstream to upstream. Station 2 (Close to Vanderhoof town) is labeled Vanderhoof. Station 5 (labeled as Nautley) is just upstream of the confluence on the Nautley River. The yellow area shows the modeled region using CEQUEAU from Skins Lake Spillway (SLS) to Station 1. The computational units in CEQUEAU are “Whole Squares or CE” and “Partial Squares or CP.” Each CE, a square grid cell, can be divided into a maximum of four CPs by overlapping CEs and sub-watershed boundaries. The CPs are hydrologic response units in CEQUEAU and are shown for the main river from SLS to Station 1. The Ootsa Lake is impounded part of the Nechako River due to Kenny Dam construction which SLS controls its flow downstream, and Natalkuz Lake is the impounded part of the Nechako River immediately upstream of Kenny Dam.

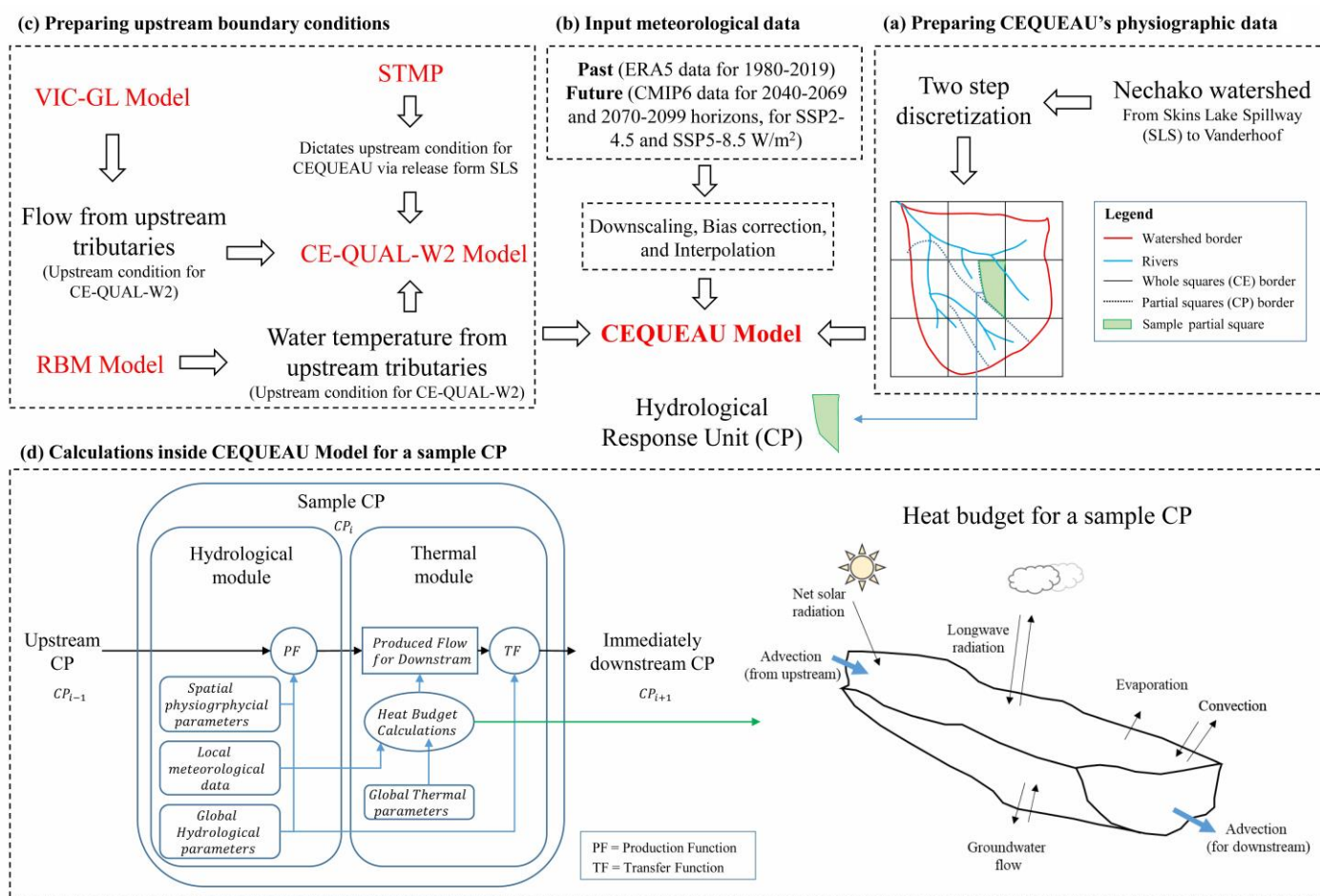
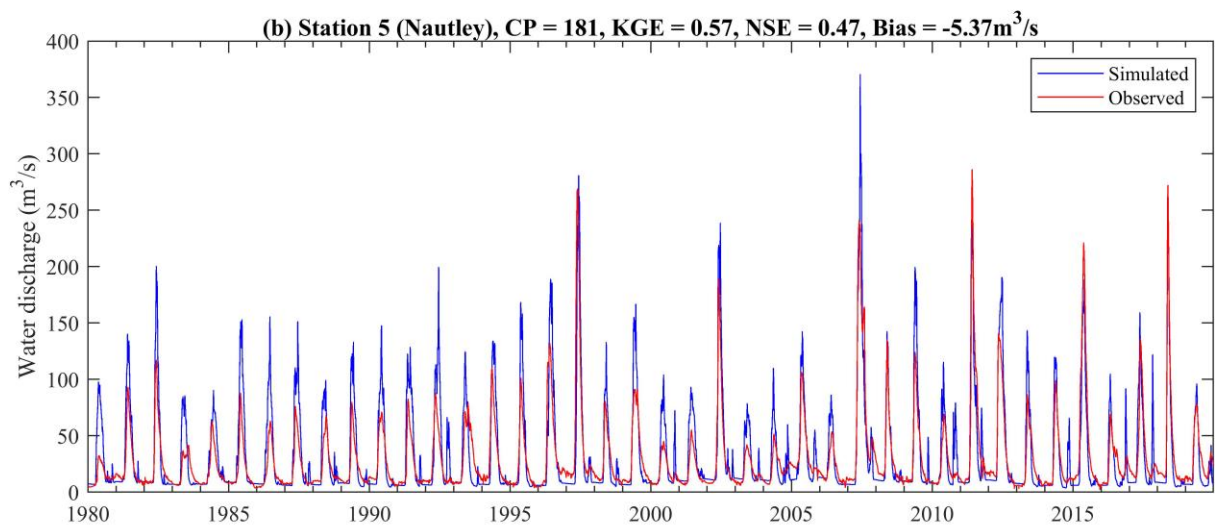
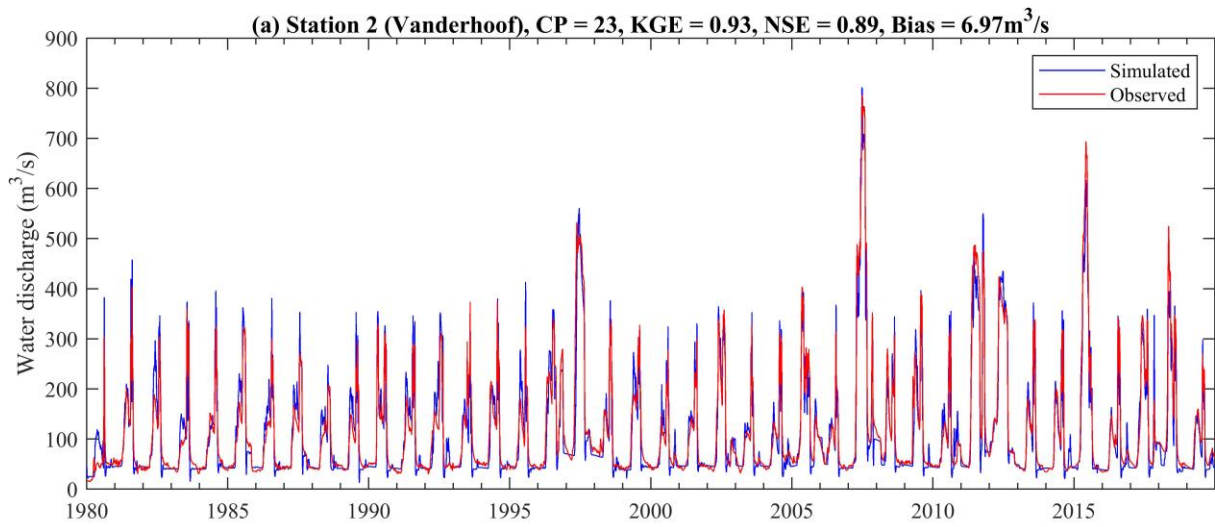


Fig. 2 Schematic representation of steps, concepts, and models to set up the CEQUEAU model in this study, including (a) physiographical data for the watershed, whole squares, and partial squares; (b) input meteorological data (precipitation, min and max air temperature, vapor pressure, cloud cover, net solar shortwave radiation), (c) the models incorporated to prepare upstream boundary condition for CEQUEAU; (d) structure of a sample partial square (CP) which is a hydrological response unit for which both hydrological and thermal budgets are computed. The core of the hydrological module is the Production Function (PF) and Transfer Function (TF), which calculates available water inside each CP and subsequent routing downstream. The thermal module calculates the heat budget using available water inside each CP.

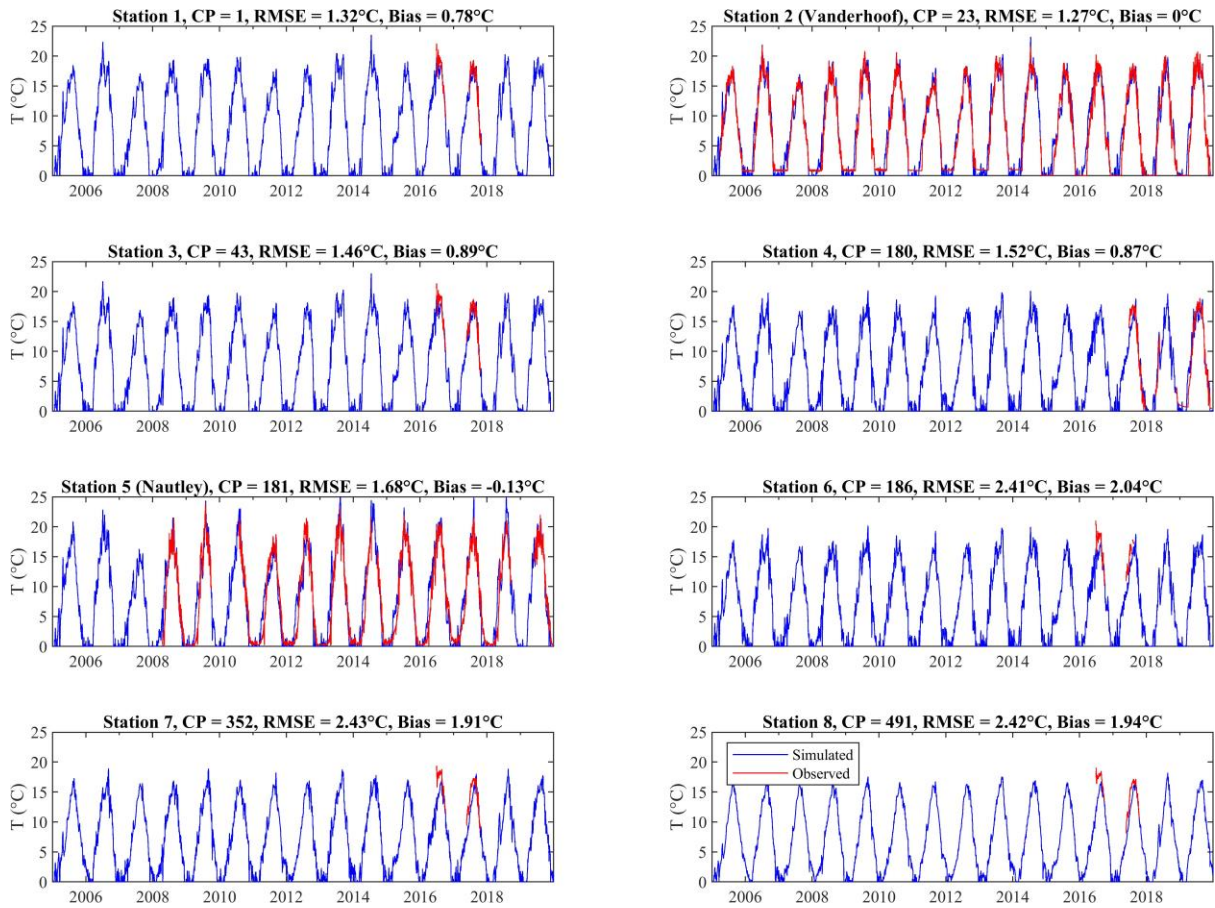


803

804

805

Fig. 3 Simulated and observed flows using the calibrated model for Vanderhoof and Nautley stations for the June-September period



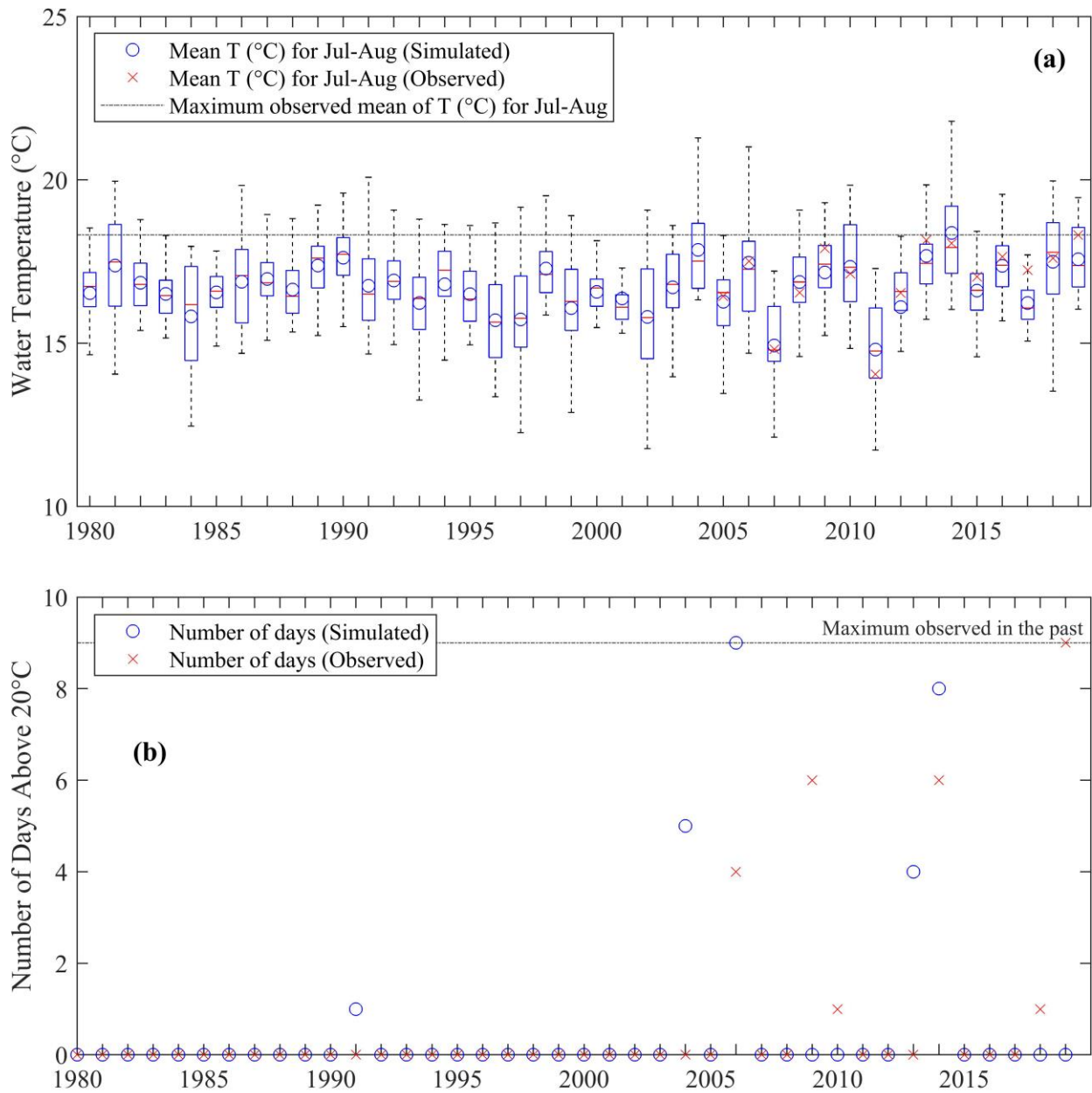
806

807

808

Fig. 4 The simulated (blue) and observed (red) water temperature time series for each station using the multisite calibration approach for the June-September period

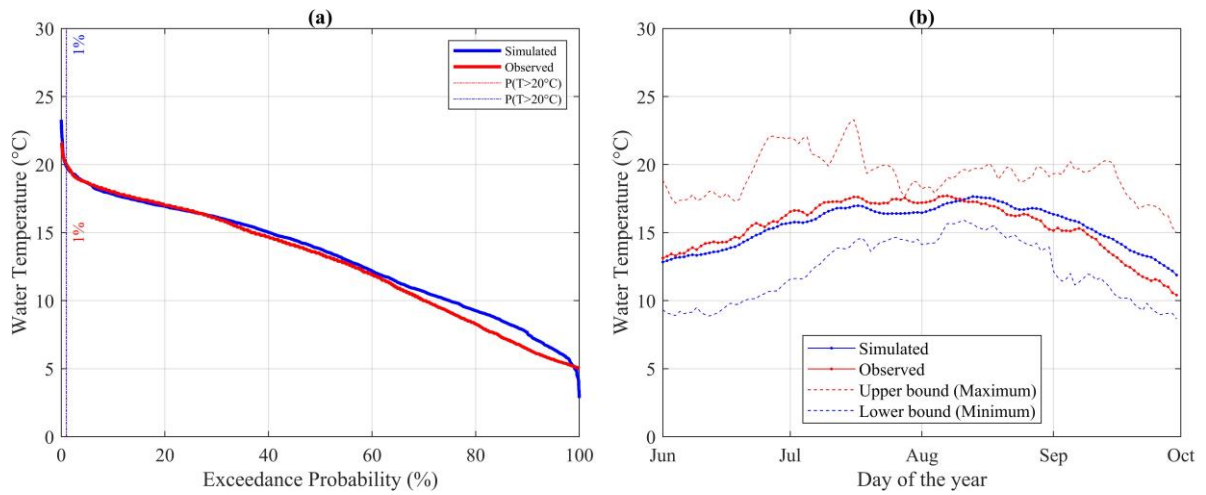
809



810

811 **Fig. 5** (a) The yearly range [for July-August only] of simulated water temperature variability is shown using
 812 boxplots for the Vanderhoof station's baseline period 1980-2019. The red line represents the median value, and
 813 the blue circles show the mean simulated value. The upper and lower limits of the boxes show the 25th and 75th
 814 percentiles, respectively, and the whiskers show the most extreme data. The mean annual temperature of the
 815 observed data is shown with the red crosses (x) (2005-2019 only). (b) Red crosses and blue circles show the
 816 annual number of days on which the mean daily temperature exceeds the critical limit of 20°C for simulated and
 817 observed time series, respectively. The horizontal dotted line shows the maximum number of observed days
 818 above 20°C in a year, equal to 9 days

819



820

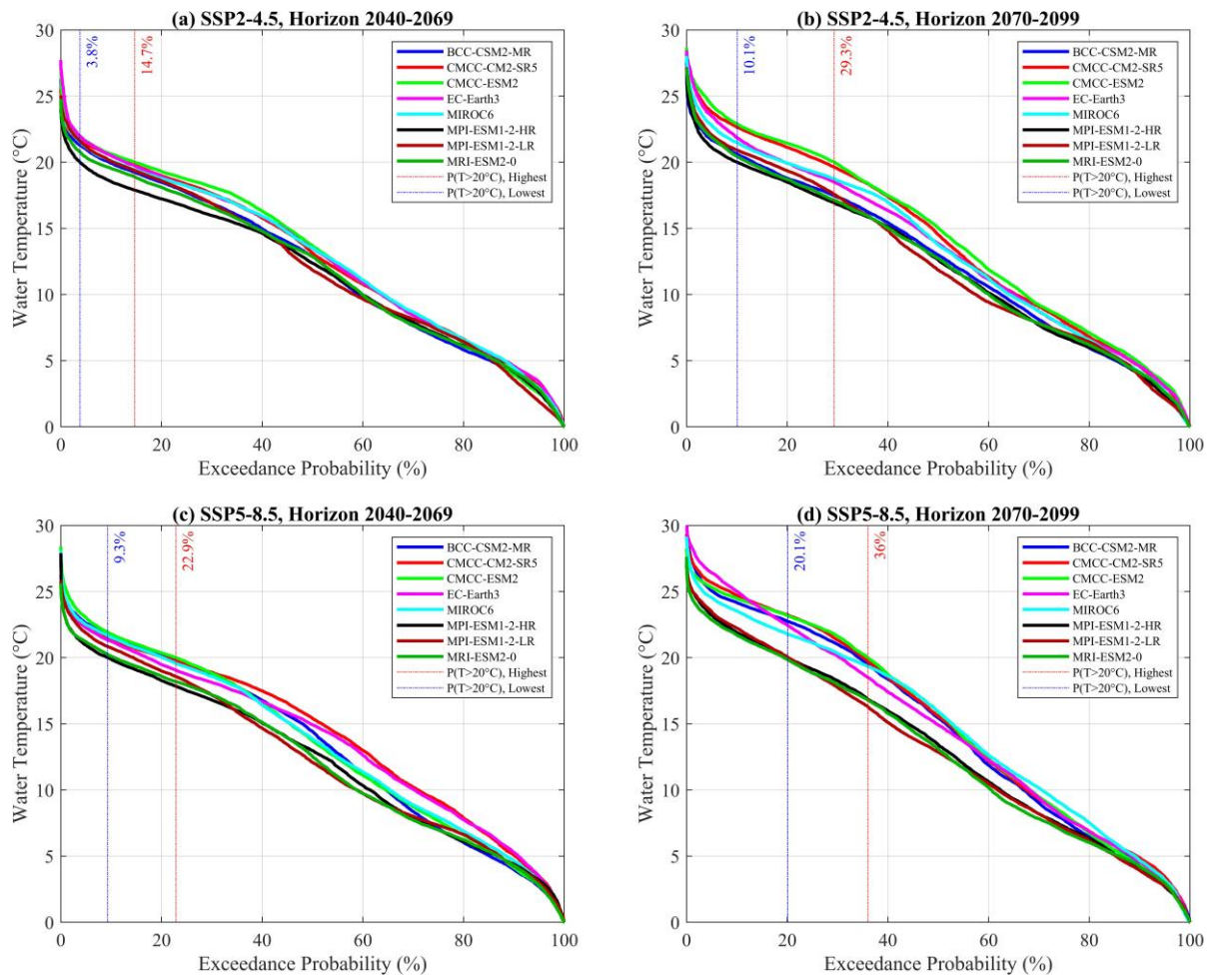
821

822

823

Fig. 6 (a) Duration curve of baseline (1980-2019) simulated data and observed water temperatures at the Vanderhoof station (b) Water temperature timing for the warm season (June-September) for observed and simulated time series together with the lower and upper boundary of simulated values

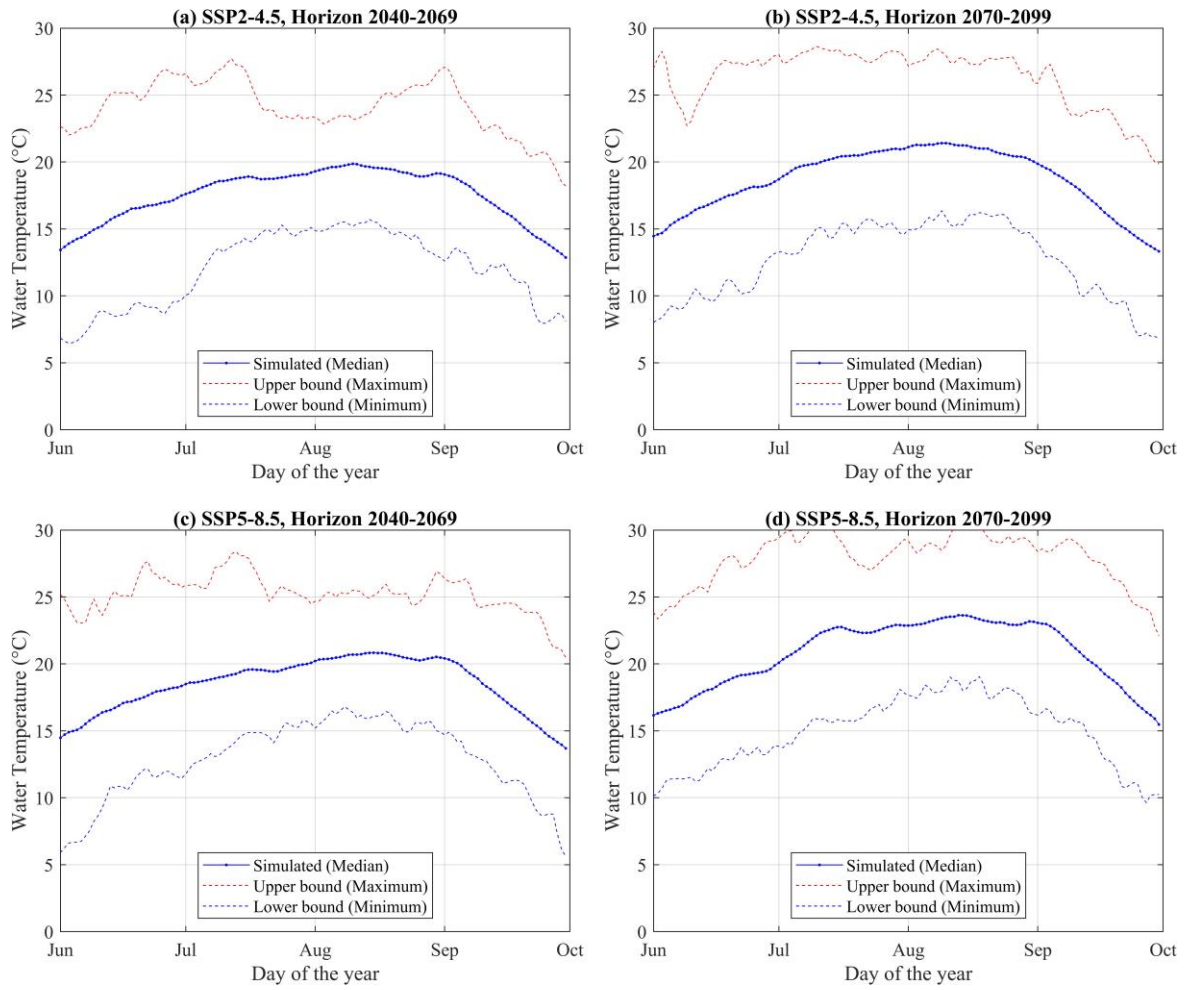
824



825

826 **Fig. 7** Duration curve of simulated data using eight climate models and their median for SSPs 4.5 and 8.5W/m²
 827 and for the 2040-2069 and 2070-2099 time horizons at the Vanderhoof station. The models with the lowest and
 828 highest exceedance probabilities were used to calculate the minimum and maximum exceedance probabilities
 829 depicted on the graphs.

830



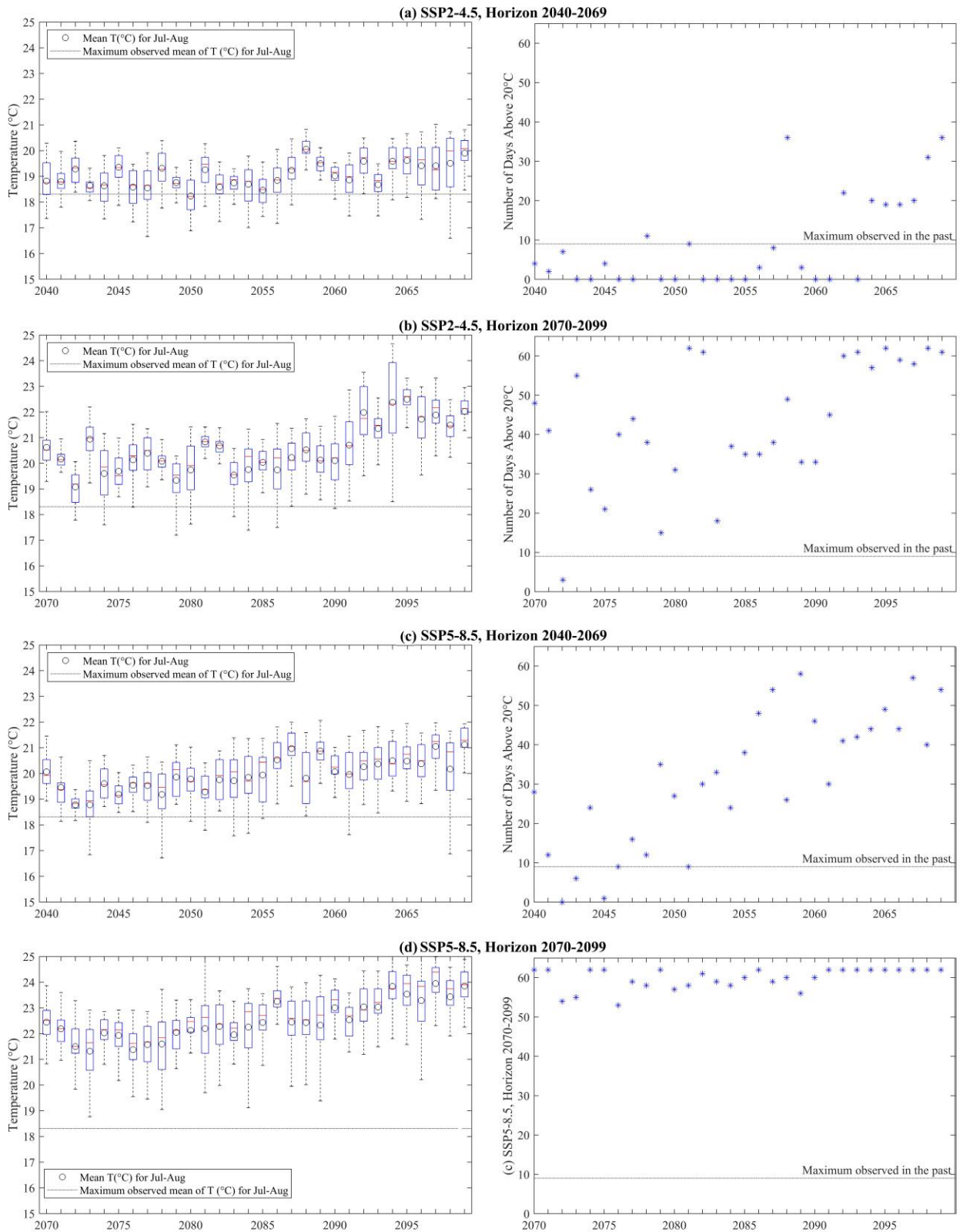
831

832

833

834

Fig. 8 High water temperatures timing for the June-September period for the simulated time series in the future, together with the lower and upper boundary of simulated values



835

836
837
838
839
840
841

Fig. 9 The yearly range of water temperature variability is shown using boxplots for two-time horizons and two SSPs. The red line represents the median multi-model value, and the black circles show the mean multi-model simulated value. The upper and lower limits of the boxes show 25th and 75th percentiles, respectively, and the whiskers show the most extreme data. The horizontal dotted line on the left panels shows the maximum observed mean of temperatures for July-August months in the past. Blue asterisks on the right-side plots show the annual number of days on which the temperature exceeds the critical limit of 20°C for simulated and

842 observed time series using multi-model median values. The horizontal dotted line shows the maximum number
843 of observed days above 20°C in a year, which occurred during the 2005-2019 period and is equal to 9 days.

844

Supplementary Files

This is a list of supplementary files associated with this preprint. Click to download.

- [6SupplementaryInformation22082023.docx](#)